Remote sensing-based determination of understory grass greening stage over boreal forest

Quazi K. Hassan
K. Mahmud Rahman

SPIE

Remote sensing-based determination of understory grass greening stage over boreal forest

Quazi K. Hassan and K. Mahmud Rahman

University of Calgary, Department of Geomatics Engineering, 2500 University Drive NW,
Calgary, Alberta, Canada T2N 1N4
qhassan@ucalgary.ca

Abstract. Our objective was the determination of understory grass greening stage (GGS: defined as the date when 75% of the grass in the surrounding area of a particular location would be green) using remote sensing data over the boreal-dominant forested regions in the Canadian province of Alberta. We used moderate resolution imaging spectroradiometer (MODIS)-derived accumulated growing degree days (AGDD) and normalized difference water index (NDWI) with ground-based understory GGS observations at approximately 120 lookout tower sites during the period 2006 to 2008. During 2006, we extracted the temporal dynamics of AGDD/NDWI at the lookout tower sites and determined the best thresholds (i.e., 90 degree-days for AGDD and 0.45 for NDWI). These AGDD/NDWI thresholds were then implemented during 2007 and 2008; and observed that AGDD had better prediction capabilities in comparison to NDWI (i.e., ~94% and ~65% of the incidents fall within ± 2 periods or ± 16 days of deviations with the ground-based understory GGS observations using AGDD and NDWI thresholds, respectively). The outcomes would potentially be useful in understanding availability of food and habitat for wildlife species/animals; microclimatic environment, composition, and diversity of plant community; and forest fire danger and fire behavior in case of fire occurrences.

1 Introduction

Understory vegetation (e.g., grasses, herbs, shrubs, etc.) is the layer of foliage below the forest canopy. In general, climatic conditions largely influence the phenology (i.e., the seasonal dynamics) associated with understory vegetation. In fact, the study of such understory phenology is very important in understanding: (1) microclimatic environment, composition, and diversity of plant community,[1–3] (2) overstory succession and nutrient cycling,[4–6] and (3) sources of food and habitat for wildlife species/animals.[7] Here, we intend to focus on one of the important understory phenological stages over boreal forest regions, i.e., understory grass greening (GGS: defined as the date when 75% of the grasses in the surrounding area of a particular location are green).[8] In addition to the above-mentioned importance of understory phenology, GGS is also important in predicting forest fire danger (i.e., probability of fire occurrence) and fire behavior in case of fire occurrences.[8]

The most common and widely employed method to study understory phenology is the use of ground-based observations. For example: (1) Richardson and O'Keefe[9] analyzed the long-term Harvard forest phenology record to decide differences in spring and autumn phenology of understory species (i.e., shrub and herbs) in central Massachusetts, USA, using photosynthetically active radiation (PAR); (2) Kudo et al.[10] predicted the understory (i.e., herbaceous) phenology during spring, early summer, and late summer bloomers at Tomakomai Experimental Forest of Hokkaido University in northern Japan using air temperature and PAR; and (3) Liang et al.[11] determined spring time understory (i.e., grasses and herbs) greenness at Chequamegon National

Forest in northern Wisconsin, USA, using ground-based air temperature, relative humidity, and digital photographs. In the Canadian province of Alberta, the Alberta Environment and Sustainable Resource Development has been estimating understory grass greening stages over the boreal dominant forested regions using visual observations at approximately 120 lookout tower sites across the landscape.[8] In general, the above-mentioned methods could find the understory phenology; however, not useful for determining the dynamics over a large geographic area.

In order to address the above mentioned limitation, remote sensing-based methods could be useful due to their ability to provide information over large and remote areas in the landscape. However, earlier studies have used remote sensing methods only in mapping the spatial distribution of the understory vegetation. For example: (1) Tuanmu et al.[12] mapped understory bamboo using moderate resolution imaging spectroradiometer (MODIS)-derived wide dynamic range vegetation index (WDRVI) at the Chinese Wolong Nature Reserve; and (2) Wilfong et al.[13] mapped understory vegetation (an invasive shrub) using LANDSAT ETM+–derived normalized difference vegetation index (NDVI) and other vegetation indices [simple ratio (SR), enhanced vegetation index (EVI), visible atmospherically resistant index (VARI), soil adjusted vegetation index (SAVI), normalized difference moisture index (NDMI), etc.] over southwestern Ohio and Indiana, USA. The mapping of understory vegetation phenology builds on these earlier mapping experiments, adding an analysis of change in the growth stage. In order to accomplish this, we chose to employ the normalized difference water index (NDWI: a measure of water content in the vegetation), because it has demonstrated better prediction capability in determining the vegetation green up stages independent of the snow conditions (i.e., common over boreal forested regions).[14,15]

As climatic variables (in particular to temperature) largely control vegetation growth, remote sensing-based surface temperature regimes have also been used in vegetation phenological studies. For example: (1) Zhang et al.[16] determined the vegetation green-up onset using MODIS-based surface temperature (T_S) and vegetation indices (i.e., NDVI and EVI) over northern mid-to-high latitudes (i.e., between 35°N and 70°N); (2) Hanes and Schwartz[17] modeled deciduous phenology using MODIS-based T_S and leaf area index in the Chequamegon National Forest in northern Wisconsin, USA; and (3) Hassan and Rahman[18] determined deciduous phenology using MODIS-based T_S and EVI-images over boreal-dominant regions in Alberta, Canada. As the use of temperature-derived predictors has not been widely explored, we opted to apply the accumulated growing degree days (AGDD)-based method (i.e., favorable temperature regime for plant growth) described in Ref. 18 in determining the understory phenology.

In this paper, our overall goal was to determine the understory GGS using MODIS-derived predictors of AGDD and NDWI over the boreal-dominant forested regions in the Canadian province of Alberta. The specific objectives were: (1) determination of threshold-values for both AGDD and NDWI for predicting understory GGS at the lookout tower sites during 2006 (see Fig. 1 for location information); (2) implementation of the determined threshold values in the first objective to evaluate their performances using an independent dataset collected during 2007 to 2008; and (3) generation of understory GGS maps using the best predictor obtainable from the first objective.

2 Method

2.1 General Description of the Study Area

In this study, we considered the forested regions within the Canadian province of Alberta (i.e., between 49°N to 60°N latitude, and 110°W to 120°W longitude; see Fig. 1). This region experiences relatively short summers, long and cold winters with annual temperature varying from −7.1°C to 6.0°C, and the average annual precipitation between 260 and 1710 mm.[19] It has a wide variety of land covers with various types of understory (i.e., shrubs-herbs, lichen, sphagnum, beaked hazelnut, willow, grouse-berry, dogwood, Labrador tea, etc.).[19] Figure 1(a) shows forest dominant regions in the study area derived from a MODIS-based land cover map at
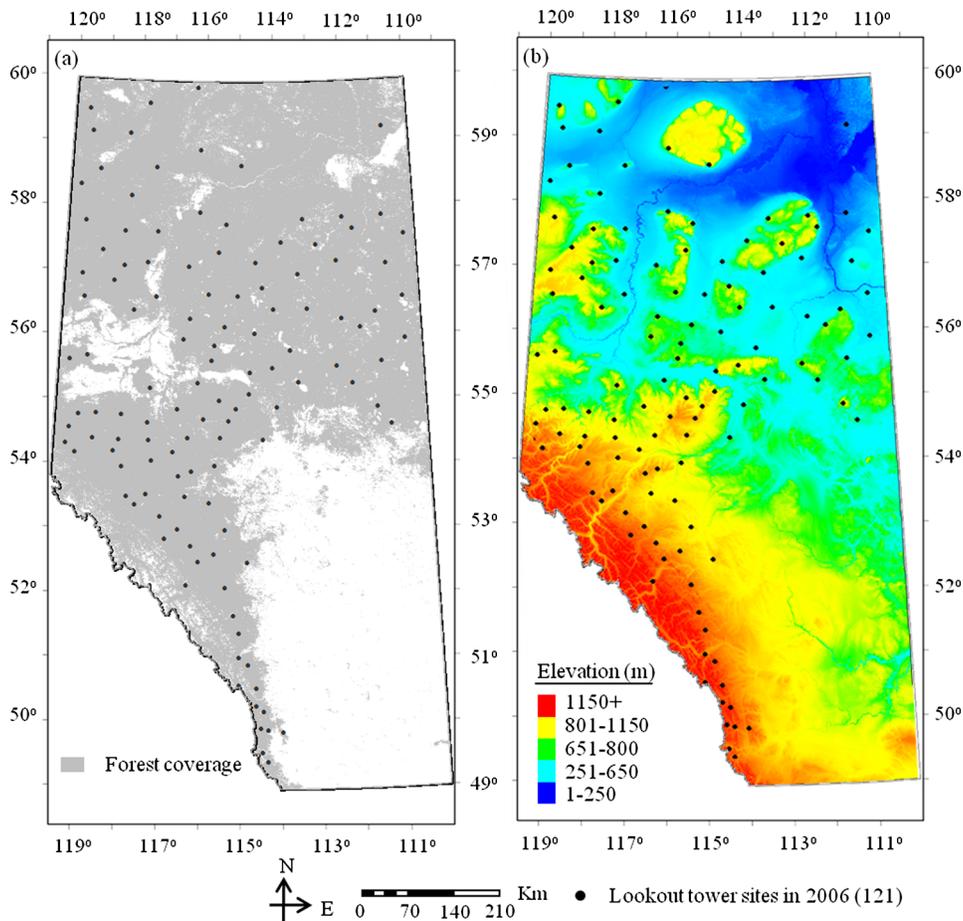
Fig. 1 Location of the ground-based understory grass greening stage (GGS) observation lookout tower sites shown over: (a) forest cover map; and (b) digital elevation model of the study area.

a spatial resolution of 500 m with the locations of the lookout tower sites operated during 2006 (where we acquired the understory GGS records).

2.2 Data Requirements and Processing

In this study, primarily we used MODIS-based data, i.e., (1) MODIS-derived GDD/AGDD maps at 500 m resolution during the 2006 to 2008 period available from an earlier study;[18] (2) eighty-one (81) 8-day composites of surface reflectance data (MOD09A1 v.005) at 500 m spatial resolution to calculate NDWI during the growing season (i.e., April to October) for the period of 2006 to 2008; and (3) an annual land cover map (MCD12Q1 v.005) at 500 m resolution for the year 2008 for delineating the forested regions. Apart from these, we also acquired ground-based observations for understory GGS at 121, 122, and 120 lookout tower sites (see Fig. 1 for location information) during 2006, 2007, and 2008, respectively; and used them to calibrate and validate the MODIS-based predictions. Note that Alberta Environment and Sustainable Resource Development collected these data using visual observations over an area of approximately 100×100 m around the lookout tower sites (Dylan Heerema: a veteran lookout tower operator, personal communication). The lookout tower operators recorded these data on a daily basis and reported in the form of day of year (DOY: 1 to 365 or 366 depending on the leap year); thus, we transformed them into 8-day period to align with 8-day composites of MODIS-based data using the following equation described in Ref. 15:

$$P = \left(\frac{\text{DOY} - 1}{8} \right) + 1, \tag{1}$$

where P (=1 to 46) is the period of MODIS-based 8-day composites throughout the year. Note that the value of P should always be an integer, e.g., $P = 20$ if Eq. (1) calculates the magnitude of P in between 20.125 and 20.875.

2.2.1 Generation of GDD/AGDD

The GDD/AGDD maps at 8-day intervals were previously generated using: (1) MODIS-based 8-day composites of T_S images at 1 km resolution (i.e., MOD11A2 v.005), (2) EVI images at 500 m resolution derived from MODIS-based surface reflectance data, and (3) 8-day mean air temperature ($\bar{T}_a$) at 182 weather stations across the study area calculated from their respective daily values. A brief description about the methodological steps would be as follows (see Ref. 18 for detailed information): (1) generation of $\bar{T}_a$ at 1 km resolution from T_S images using an empirical linear relationship (i.e., $\bar{T}_a = 0.61 * T_S + 103.66$, with temperatures in Kelvin); (2) calculation of GDD images at 1 km resolution by subtracting a base temperature (=278.15 K; assumed as the required minimum temperature for the startup of understory GGS) from $\bar{T}_a$; (3) generation of GDD images at 500 m resolution by fusing EVI images with the GDD images at 1 km resolution using the data fusion method described in Ref. 20. Mathematically, the data fusion would be as follows:

$$\text{GDD}_{500\text{ m}} = \frac{\text{EVI}_{\text{ins}}}{\text{EVI}_{\text{avg}}} \times \text{GDD}_{1\text{ km}}, \tag{2}$$

where EVI_{ins} is the instantaneous value of EVI at the center of a 3×3 moving window; and EVI_{avg} is the average value of all the EVI values within the moving window. The ratio between EVI_{ins} and EVI_{avg} acts as a weighted-function in calculating GDD at 500 m resolution; and (4) finally, calculation of AGDD images at 500 m by summing the GDD at 500 m resolution at each period[18] as follows:

$$\text{AGDD} = \sum_{i=1}^{n} (8 \times \text{GDD}_{500\text{ m}}), \tag{3}$$

where i is the first 8-day period of the growing season; and n (=1 to 27) is the 8-day period of interest during the growing season.

2.2.2 Generation of NDWI

We used MODIS-based 8-day composites of surface reflectance data to calculate NDWI according to the following equation described in Ref. 21:

$$\text{NDWI}_{2.13\ \mu\text{m}} = \frac{\rho_{\text{NIR}} - \rho_{\text{SWIR}_{\text{at}2.13\ \mu\text{m}}}}{\rho_{\text{NIR}} + \rho_{\text{SWIR}_{\text{at}2.13\ \mu\text{m}}}}, \tag{4}$$

where ρ is the surface reflectance for the NIR (near infrared) and SWIR (short wave infrared; 2.13 μm) spectral bands.

2.3 Determining Threshold for Understory GGS and its Validation

At the lookout tower sites (where the understory GGS records were available), we extracted both of the AGDD and NDWI-values during the period of 2006 to 2008. To determine and validate the predictor-specific thresholds, we divided these datasets into two groups for calibration (consisting of all data acquired during 2006, which would be ~34% of the entire dataset) and validation (consisting of all data acquired during 2007 to 2008, which would be ~66% of the entire dataset). In the calibration phase (i.e., determining the understory GGS threshold), there were two steps. First, we computed an average and standard deviation for both of the AGDD and NDWI-values during the understory GGS period. Then we considered these average values as initial threshold values for understory GGS, where equal or greater amount of AGDD

and NDWI would be the least requirement for understory GGS occurrence. Second, we varied the initial thresholds over a range of "±1 standard deviation" in increments of one-third standard deviation in order to determine the predictor-specific best thresholds for understory GGS. We selected the best thresholds as values providing the best agreement between predicted and ground-based observations of understory GGS. Note that we used "−" and "+" signs for premature and late predictions, respectively, compared to the ground-based understory GGS periods throughout the remaining article. For example, the 0, −1, and +1 period of deviation meant that the: (1) MODIS-based prediction and ground-based observation fell in the same period, (2) MODIS-based prediction was 1 period earlier than that of ground-based observation, and (3) MODIS-based prediction was 1 period delayed from that of ground-based observation, respectively.

In the validation phase, we employed the best thresholds for both AGDD and NDWI in predicting the understory GGS during 2007 to 2008. Also, we computed the deviations between the predicted and ground-based observed GGS periods to evaluate the effectiveness of these thresholds.

Executing both of the calibration and validation phases allowed identification of the better predictor (i.e., either AGDD or NDWI). As such, we employed the best threshold of the better predictor in generating the understory GGS over the forested areas shown in Fig. 1(a).

3 Results

3.1 Determining AGDD Threshold for Understory GGS and its Validation

Figure 2(a) shows the averaged temporal trend of AGDD (observed at all the 121 lookout tower sites), and the relative frequency distribution of the individual AGDD thresholds during 2006. During the average ground-based understory GGS period [shown with the vertical dotted-line; see Fig. 2(a)], we found that the initial threshold of AGDD was 128 degree-days with a standard deviation of ±48 degree-days. Note that ~89% of the understory GGS incidents occurred within the bound of "initial threshold ±1 standard deviation" (i.e., ~60 to 195 degree-days) [see Fig. 2(b)]. In this range, we found that the AGDD threshold of 90 was optimal, demonstrating reasonable agreement (i.e., 31.4%, 71.9%, and 90.1% agreements at 0, ±1, and ±2 periods of deviations, respectively) in relation to the ground-based understory GGS observations (see Table 1). Thus, we implemented the best AGDD threshold (i.e., 90 degree-days) during 2007 to 2008 at the lookout tower sites (see Table 2). With this threshold, a significant number of understory GGS events occurred within ±2 periods of deviations of the ground-based observations (i.e., 94.3% in 2007; 94.2% in 2008; and 94.2% in 2007 to 2008 on average).

3.2 Determining of NDWI Threshold for Understory GGS and its Validation

Figure 3(a) shows the averaged temporal trend of extracted NDWI-values at all the 121 understory GGS lookout tower sites during 2006 along with the averaged ground-based understory
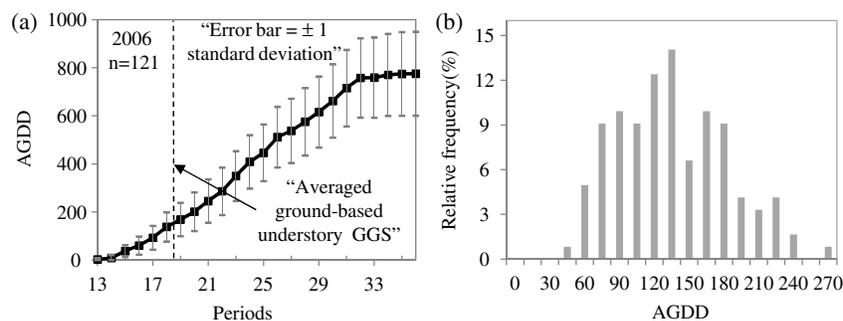

Fig. 2 Determining of AGDD threshold for understory grass greening stage (GGS); (a) average temporal trends of AGDD at all the ground-based lookout tower sites in 2006 as a function of periods; and (b) relative frequency distribution of AGDD at all the lookout tower sites.

Table 1 Implementation of different AGDD thresholds to determine the best AGDD threshold for predicting understory grass greening stage (GGS) during 2006.

AGDD threshold	% Out of 121 lookout towers (2006)							
	Deviations (in periods)							
	0	±1	±2	±3	±4	±5	±6	±7
60	19.0	53.7	79.3	94.2	100	100	100	100
75	24.0	64.2	83.5	97.5	100	100	100	100
90	31.4	71.9	90.1	98.3	100	100	100	100
105	27.3	65.0	86.8	97.5	99.2	100	100	100
120	24.0	67.8	86.0	93.4	99.2	100	100	100
135	16.5	62.0	84.3	91.7	98.3	99.2	100	100
150	19.8	56.2	78.5	89.3	96.7	99.2	100	100
165	14.0	47.9	71.1	86.0	95.0	99.2	100	100
180	9.1	41.3	63.6	82.6	92.6	99.2	100	100
195	6.6	34.7	53.7	76.0	88.4	97.5	99.2	100

GGS observed period (shown using a vertical dotted line). The initial NDWI threshold was having a value of 0.48 with a standard deviation of 0.16. In addition, the relative frequency distribution of the individual NDWI threshold values were found in the range of 0.30 to 0.65 (i.e., ∼initial threshold ± 1 standard deviation) for ∼86% of the incidents [see Fig. 3(b)]. In this range, we found that the NDWI threshold of 0.45 would be the best selection, which produced reasonable agreement (i.e., 21.5%, 56.2%, 69.4% of the incidents at 0, ±1, and ±2 periods of deviations, respectively) in comparison to the ground-based understory GGS (see Table 3). Thus, the NDWI threshold value of 0.45 was selected as the best NDWI threshold, which was also relatively close to the initial NDWI threshold of 0.48. Then we implemented the best NDWI threshold (i.e., 0.45) during 2007 to 2008 at the lookout tower sites (see Table 4). It revealed that the deviations were reasonable (i.e., ±2 periods of deviation for 63.1% of the incidents in 2007; 65.8% in 2008; and 64.5% in 2007 to 2008 on average) in comparison to the ground-based understory GGS observations.

3.2.1 Spatial dynamics of understory GGS

Between the two predictors, we found that the AGDD function with a threshold of 90 degree-days was the better one. Thus, we implemented this function in generating the spatial dynamics

Table 2 Relation between ground-based observed and AGDD-based predicted understory grass greening stage (GGS) periods at each lookout tower sites during 2007 to 2008 using the optimal AGDD threshold of 90 degree-days. The "+ve" and "−ve" signs represent positive (i.e., late) and negative (i.e., premature) predictions, respectively.

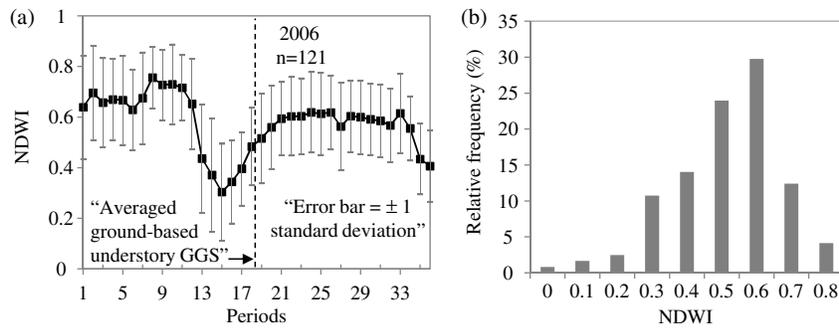| Year	No. of lookout tower sites	Deviations (in periods)					
		0	±1	±2	±3	±4	±5
2007	122	44.3	79.5	94.3	96.7	98.4	100
2008	120	35.8	73.3	94.2	99.2	100	100
2007 to 2008	121	40.1	76.4	94.2	97.9	99.2	100

Fig. 3 Determining of NDWI threshold for understory grass greening stage (GGS); (a) average temporal trends of NDWI at all the ground-based lookout tower sites in 2006 as a function of periods; and (b) relative frequency distribution of NDWI at all of the lookout tower sites.

of understory GGS over the forest dominant areas. Figure 4 shows such examples for the period 2006 to 2008. We found that most of the understory GGS (i.e., for ~68%, 82%, and 93% of the incidents during 2006, 2007, and 2008, respectively) took place during the periods 18 to 21 (i.e., 17 May to 17 June during 2006 and 2007; and 16 May to 16 June during 2008).

4 Discussion

During the calibration phase, we observed some variability associated with each of the predictors (i.e., AGDD thresholds varied between 60 and 195 degree-days for ~89% of the incidents, and NDWI thresholds between 0.30 and 0.65 for ~86% of the incidents). This variability might be associated with one or more of the following reasons: (1) in case of AGDD-based prediction, other influencing climatic factors (e.g., water stress and incident photosynthetically active radiation) were not taken into consideration; (2) in general, climatic regimes (e.g., winter temperature and summer moisture conditions) during the previous season might influence the vegetation growth over boreal forest[22] by controlling the timing of occurring a phonological stage of interest; (3) the growth dynamics of the understory vegetation might depend on disturbance regimes (e.g., fire, insect infestation) and also changes with overstory structure[23]; and (4) nutrient regimes might be variable among the lookout tower sites.

During the validation phase, we observed relatively high deviations (i.e., $> \pm 2$ periods) between the MODIS-predicted and ground-based observations for ~6% and ~35% of the

Table 3 Implementation of different NDWI thresholds to determine the best NDWI threshold for predicting understory grass greening stage (GGS) during 2006.

	% Out of 121 lookout towers (2006)								
	Deviations (in periods)								
NDWI threshold	0	±1	±2	±3	±4	±5	±6	±7	> ± 7
0.3	13.2	50.4	66.9	85.1	92.6	95.9	98.3	100	100
0.35	9.9	49.6	67.8	81.0	90.9	95.9	96.7	99.2	100
0.4	15.7	50.4	68.6	83.5	88.4	90.9	94.2	97.5	100
0.45	21.5	56.2	69.4	78.5	85.1	90.1	97.5	98.3	100
0.5	24.0	51.2	65.3	77.7	86.0	91.7	95.9	98.3	100
0.55	24.0	43.8	57.0	65.3	81.0	90.1	95.9	100	100
0.6	13.2	33.1	54.5	62.8	73.6	83.5	95.0	99.2	100
0.65	13.2	33.1	45.5	62.0	72.7	84.3	94.2	97.5	100

Table 4 Relation between ground-based observed and NDWI-based predicted understory grass greening stage (GGS) periods at each of the lookout tower sites during 2007 to 2008 using the optimal NDWI threshold of 0.45. The "+ve" and "−ve" signs represent positive (i.e., late) and negative (i.e., premature) predictions, respectively.

Year	No. of lookout tower sites	Deviations (in periods)						
		0	±1	±2	±3	±4	±5	±6
2007	122	18.9	48.4	63.1	79.5	90.2	98.4	100
2008	120	16.7	43.3	65.8	79.2	88.3	95.8	100
2007 to 2008	121	17.8	45.9	64.5	79.3	89.3	97.1	100

incidents using AGDD and NDWI thresholds, respectively. These might be related to one or a combination of the following causes: (1) due to the use of visual observations in collecting the understory GGS records, it would be possible to have variation from one to another operator;[15] (2) a single threshold for the predictor of interest would not be suitable in capturing the spatial dynamics over the study area[18,24]; and (3) in some instances, the spatial resolution of the MODIS-based predictions might not commensurate with that of the ground-based observations.

In terms of determined best thresholds (i.e., AGDD threshold of 90 degree-days, and NDWI threshold of 0.45), it was not possible to compare these as there were no similar studies found in the literature. The rationale behind better performance of AGDD-based predictions might be associated with the fact that temperature regimes would often dominate the dynamics of boreal forested regions as spring snow-melting may provide the required soil water.[25] Besides, it would not be possible to link satellite-based surface reflectance (thus, NDWI) with the understory situation due to overstory barrier/forest structure,[12] which might cause inferior NDWI-based predictions.
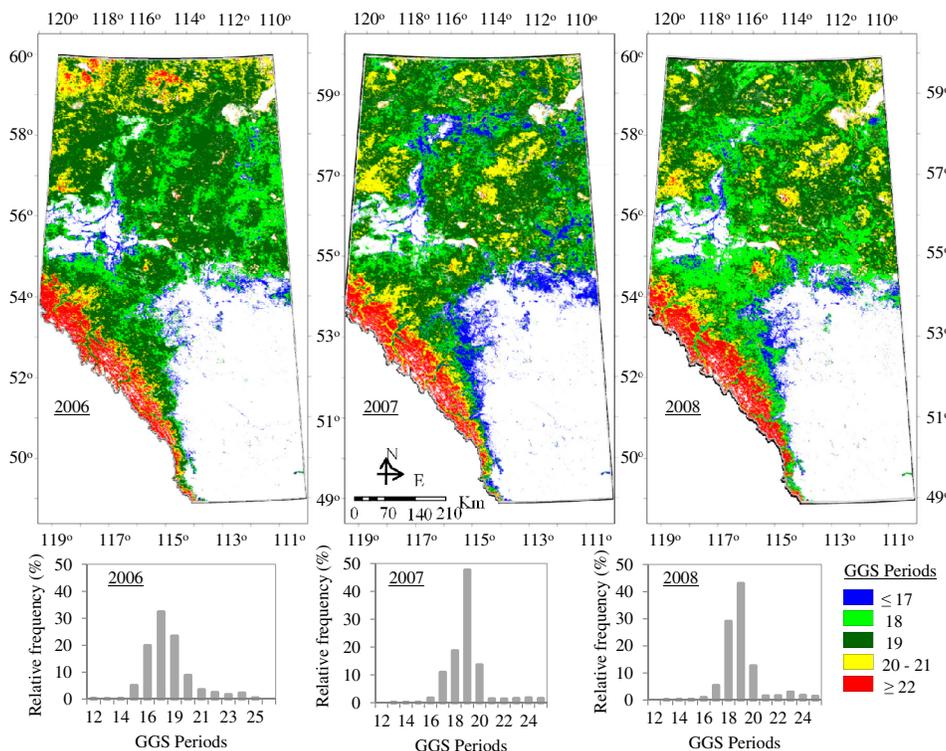

Fig. 4 Spatial dynamics for the timing of understory greening stage (GGS) in periods and its relative frequency distribution during 2006, 2007, and 2008.

In the understory GGS map, we observed some generalized spatial patterns. For example: (1) relatively early (i.e., ≤17 periods) understory GGS occurred predominantly in the southeastern fringe of the forested component of the domain, which experiences relatively warmer temperature; (2) relatively late (≥20 periods) understory GGS occurred towards the northern/high elevated/mountain area [see these areas in Fig. 1(b)]; attributed the fact that the temperature regime decreases in the northward directions in the northern hemisphere and high elevated areas.[15,26]

5 Concluding Remarks

In this paper, we evaluated the MODIS-based AGDD and NDWI in determining the understory GGS over the boreal forested regions in Alberta. Between the best thresholds of AGDD and NDWI, we found that the AGDD produced better results (i.e., ~91.9% of the incidents fall within ±2 periods or ±16 days of deviation). This work would be applicable in particular to remote areas where ground-based observations would not be possible. Despite the effectiveness of the employed method, we would strongly recommend that the AGDD threshold-value would be properly calibrated and validated prior to applying to other ecosystems.

Acknowledgments

References

1. S. E. Macdonald and T. E. Fenniak, "Understory plant communities of boreal mixedwood forests in western Canada: natural patterns and response to variable retention harvesting," *For. Ecol. Manage.* **242**(1), 34–48 (2007), http://dx.doi.org/10.1016/j.foreco.2007.01.029.
2. V. Chavez and S. E. Macdonald, "Understory species interactions in mature boreal mixedwood forests," *Botany* **88**(10), 912–922 (2010), http://dx.doi.org/10.1139/B10-062.
3. X.-T. . Lu, J.-X. Yin, and J.-W. Tang, "Diversity and composition of understory vegetation in the tropical seasonal rain forest of Xishuangbanna, SW China," *Int. J. Rev. Biol. Trop.* **59**(1), 455–463 (2011).
4. M. R. Roberts, "Response of the herbaceous layer to natural disturbance in north American forests," *Can. J. Bot.* **82**(9), 1273–1283 (2004), http://dx.doi.org/10.1139/b04-091.
5. S. A. Hart and H. Y. H. Chen, "Understory vegetation dynamics of north American boreal forests," *Crit. Rev. Plant. Sci.* **25**(4), 381–397 (2006), http://dx.doi.org/10.1080/07352680600819286.
6. F. S. Gilliam, "The ecological significance of the herbaceous layer in temperate forest ecosystems," *Biosci.* **57**(10), 845–858 (2007), http://dx.doi.org/10.1641/B571007.
7. M. C. Nilsson and D. A. Wardle, "Understory vegetation as a forest ecosystem driver: evidence from the northern Swedish boreal forests," *Fron. Ecol. Environ.* **3**(8), 421–428 (2005), http://dx.doi.org/10.1890/1540-9295(2005)003[0421:UVAAFE]2.0.CO;2.
8. Alberta Land and Forest Service, "Forest fire management terms," Forest Protection Division, p. 77 (1999), http://www.srd.alberta.ca/Wildfire/WildfireOperations/documents/ForestFireManagementTerms-Glossary-1999.pdf (17 August 2012).
9. A. D. Richardson and J. O'Keefe, "Phenological differences between understory and overstory: a case study using the long-term Harvard forest records," in *Phenology of Ecosystem Processes*, A. Noormets, Ed., pp 87–118, Springer, New York (2009).
10. G. Kudo, T. Y. Ida, and T. Tani, "Linkages between phenology, pollination, photosynthesis, and reproduction in deciduous forest understory plants," *Ecology* **89**(2), 321–331 (2008), http://dx.doi.org/10.1890/06-2131.1.
11. L. Liang, M. D. Schwartz, and S. Fei, "Photographic assessment of temperate forest understory phenology in relation to springtime meteorological drivers," *Int. J. Biometeorol.* **56**(2), 343–355 (2012), http://dx.doi.org/10.1007/s00484-011-0438-1.

12. M. Tuanmu–N et al., "Mapping understory vegetation using phenological characteristics derived from remotely sensed data," *Rem. Sens. Environ.* **114**(8), 1833–1844 (2010), http://dx.doi.org/10.1016/j.rse.2010.03.008.

13. B. N. Wilfong, D. L. Gorchov, and M. C. Henry, "Detecting an invasive shrub in deciduous forest understories using remote sensing," *Weed Sci.* **57**(5), 512–520 (2009), http://dx.doi.org/10.1614/WS-09-012.1.

14. N. Delbart et al., "Determination of phenological dates in boreal regions using normalized difference water index," *Rem. Sens. Environ.* **97**(1), 26–38 (2005), http://dx.doi.org/10.1016/j.rse.2005.03.011.

15. N. S. Sekhon, Q. K. Hassan, and R. W. Sleep, "Evaluating potential of MODIS-based indices in determining "snow gone" stage over forest-dominant regions," *Rem. Sens.* **2**(5), 1348–1363 (2010), http://dx.doi.org/10.3390/rs2051348.

16. X. Zhang et al., "Climate controls on vegetation phenological patterns in northern mid- and high latitudes inferred from MODIS data," *Glob. Chang. Biol.* **10**(7), 1133–1145 (2004), http://dx.doi.org/10.1111/j.1529-8817.2003.00784.x.

17. J. M. Hanes and M. D. Schwartz, "Modeling land surface phenology in a mixed temperate forest using MODIS measurements of leaf area index and land surface temperature," *Theor. Appl. Climatol.* **105**(1–2), 37–50 (2010), http://dx.doi.org/10.1007/s00704-010-0374-8.

18. Q. K. Hassan and K. M. Rahman, "Applicability of remote sensing-based surface temperature regimes in determining deciduous phenology over boreal forest," *J. Plant. Ecol.* **6**(1), 84–91 (2013), http://dx.doi.org/10.1093/jpe/rts010.

19. D. J. Dowing and W. W. Pettapiece, Eds., *Natural Regions and Subregions of Alberta*, Publication T/852, Natural Regions Committee, Government of Alberta, Alberta, Canada (2006).

20. Q. K. Hassan, C. P. Bourque–A, and F. Meng–R, "Application of Landsat-7 ETM+ and MODIS products in mapping seasonal accumulation of growing degree days at an enhanced resolution," *J. Appl. Rem. Sens.* **1**(1), 013539 (2007), http://dx.doi.org/10.1117/1.2800284.

21. D. Chen, J. Huang, and T. J. Jackson, "Vegetation water content estimation for corn and soybeans using spectral indices derived from MODIS near- and short-wave infrared bands," *Rem. Sens. Environ.* **98**(2–3), 225–236 (2005), http://dx.doi.org/10.1016/j.rse.2005.07.008.

22. J. Huang et al., "Radial growth response of four dominant boreal tree species to climate along a latitudinal gradient in the eastern Canadian boreal forest," *Glob. Chang. Biol.* **16**(2), 711–731 (2010), http://dx.doi.org/10.1111/j.1365-2486.2009.01990.x.

23. A. W. D'Amato, D. A. Orwig, and D. R. Foster, "Understory vegetation in old-growth and second-growth Tsuga canadensis forests in western Massachusetts," *For. Ecol. Manage.* **257**(3), 1043–1052 (2009), http://dx.doi.org/10.1016/j.foreco.2008.11.003.

24. H. Li, X. Wang, and A. Hamann, "A genetic adaptation of aspen (Populus tremuloides) populations to spring risk environments: a novel remote sensing approach," *Can. J. For. Res.* **40**(11), 2082–2090 (2010), http://dx.doi.org/10.1139/X10-153.

25. G. E. Jones and B. M. Cregg, "Screening exotic firs for the midwestern United States: interspecific variation in adaptive traits," *HortSci.* **41**(2), 323–328 (2006).

26. Q. K. Hassan et al., "Spatial mapping of growing degree days: an application of MODIS-based surface temperatures and enhanced vegetation index," *J. Appl. Rem. Sens.* **1**(1), 013511 (2007), http://dx.doi.org/10.1117/1.2740040.

Quazi K. Hassan received his PhD degree in remote sensing and ecological modelling from University of New Brunswick, Canada. He is currently an assistant professor in the Department of Geomatics Engineering at the University of Calgary. His research interests include the integration of remote sensing, environmental modeling, and GIS in addressing environmental issues.

K. Mahmud Rahman received his MSc degree in geomatics engineering from University of Calgary in 2011. His research focuses on the use of remote sensing-based vegetation phenology (e.g., deciduous leaf out, leaf fall, understory green up, etc.) in boreal forested regions of Alberta.